

Looking for Lorentz invariance violation (LIV) in the latest long baseline accelerator neutrino oscillation data

Ushak Rahaman¹

¹*Centre for Astro-Particle Physics (CAPP) and Department of Physics,
University of Johannesburg, PO Box 524, Auckland Park 2006, South Africa*

(Dated: Received: date / Revised version: date)

Abstract

In this paper, we have analysed the latest data from NO ν A and T2K with the Lorentz invariance violation along with the standard oscillation hypothesis. We have found that the NO ν A data cannot distinguish between the two hypotheses at 1σ confidence level. T2K data and the combined data analysis excludes standard oscillation at 1σ . All three cases do not have any hierarchy sensitivity when analysed with LIV. There is a mild tension between the two experiments, when analysed with LIV, as θ_{23} at NO ν A best-fit is at higher octant but the same for T2K is at lower octant. The present data from accelerator neutrino long baseline experiments lose octant determination sensitivity when analysed with LIV. The tension between the two experiments is also reduced when the data are analysed with LIV.

| Parameters | NH | IH |
|---|---------------------------|----------------------------|
| $\theta_{12}/^\circ$ | $33.44^{+0.77}_{-0.74}$ | $33.45^{+0.78}_{-0.75}$ |
| $\theta_{23}/^\circ$ | $49.2^{+0.9}_{-1.2}$ | $49.3^{+0.9}_{-1.1}$ |
| $\theta_{13}/^\circ$ | $8.57^{+0.12}_{-0.12}$ | $8.60^{+0.12}_{-0.12}$ |
| $\delta_{CP}/^\circ$ | 197^{+24}_{-24} | 282^{+26}_{-30} |
| $\frac{\Delta_{21}}{10^{-5} \text{eV}^2}$ | $7.42^{+0.21}_{-0.20}$ | $7.42^{+0.21}_{-0.20}$ |
| $\frac{\Delta_{3l}}{10^{-3} \text{eV}^2}$ | $2.517^{+0.026}_{-0.028}$ | $-2.498^{+0.028}_{-0.028}$ |

TABLE I: Global best-fit values of neutrino oscillation parameters [7, 8]. $\Delta_{3l} = \Delta_{31} > 0$ ($\Delta_{32} < 0$) for NH (IH).

I. INTRODUCTION

The three flavour neutrino oscillation phenomenon is parameterised by the unitary Pontecorvo-Maki-Nakagawa-Sakata (PMNS) mixing matrix:

$$U = \begin{bmatrix} c_{13}c_{12} & s_{12}c_{13} & s_{13}e^{-i\delta_{CP}} \\ -s_{12}c_{23} - c_{12}s_{23}s_{13}e^{i\delta_{CP}} & c_{12}c_{23} - s_{12}s_{23}s_{13}e^{i\delta_{CP}} & s_{23}c_{13} \\ s_{12}s_{23} - s_{13}c_{12}c_{23}e^{i\delta_{CP}} & -c_{12}s_{23} - s_{13}c_{23}s_{12}e^{i\delta_{CP}} & c_{23}c_{13} \end{bmatrix}, \quad (\text{I.1})$$

where $c_{ij} = \cos \theta_{ij}$ and $s_{ij} = \sin \theta_{ij}$. The neutrino oscillation probabilities depend on three mixing angles: θ_{12} , θ_{13} , and θ_{23} ; two independent mass squared differences: $\Delta_{21} = m_2^2 - m_1^2$ and $\Delta_{31} = m_3^2 - m_1^2$, where m_1 , m_2 and m_3 are the masses of the neutrino mass eigenstates ν_1 , ν_2 and ν_3 respectively; and a CP violating phase: δ_{CP} . Among these parameters, θ_{12} and Δ_{21} have been measured in solar neutrino experiments [1, 2]. $\sin^2 2\theta_{23}$ and $|\Delta_{31}|$ has been obtained by measuring the ν_μ survival probabilities in accelerator neutrino long baseline experiment MINOS [3]. Recently reactor neutrino experiments have measured non-zero value of θ_{13} [4–6]. In table I, we have noted down the current best-fit values along with the 1σ uncertainties of the oscillation parameters.

The current unknowns are the sign of Δ_{31} , octant of θ_{23} and the CP violating phase δ_{CP} . There can be two possible mass orderings for the masses of the neutrino mass eigenstates, depending on the sign of Δ_{31} : normal hierarchy (NH), which implies $m_3 \gg m_2 > m_1$, and inverted hierarchy (IH), which implies $m_2 > m_1 \gg m_3$ [9]. It is expected that the current

accelerator based long baseline neutrino oscillation experiments NO ν A [10] and T2K [11] will measure these unknowns by measuring the $\nu_\mu \rightarrow \nu_e$ oscillation probabilities in presence of matter effect. Recently both the experiments have published their latest analysis. The best-fit values for NO ν A is $\sin^2 \theta_{23} = 0.57_{-0.03}^{+0.04}$ and $\delta_{CP} = 0.82\pi$ for NH [12]. For T2K, the best-fit values are $\sin^2 \theta_{23} = 0.53_{-0.04}^{+0.03}$ for both mass hierarchies, and $\delta_{CP}/\pi = -1.89_{-0.58}^{+0.70}$ ($-1.38_{-0.54}^{+0.48}$) for normal (inverted) hierarchy [13]. Therefore, there is a moderate tension between the outcomes of the two experiments. The measured best-fit δ_{CP} values of both the experiments are far apart. Moreover, there is no overlap between the allowed regions on $\sin^2 \theta_{23} - \delta_{CP}$ plane at 1σ confidence level (C.L.). Although the individual experiments prefer NH over IH, their combined analysis has the best-fit point at IH [14].

Apart from the unknown standard oscillation parameters, these experiments will also investigate about the possibility of beyond standard model (BSM) physics. A large number of studies have been done about exploring BSM physics with long baseline neutrino oscillation experiments [15]. Recently non-unitary neutrino mixing [16] and non-standard neutrino interaction during propagation through matter [17, 18] have been used to resolve the tension between NO ν A and T2K. It is important to test other BSM physics models to resolve the tension as well.

Neutrino oscillation requires neutrinos to be massive albeit extremely light. This curious and interesting characteristic makes neutrino oscillation the first experimental signature of BSM physics. Without loss of any generality, SM can be considered as the low energy effective theory derived from a more general theory governed by Planck mass ($M_P \simeq 10^{19}$ GeV). This more fundamental theory unifies gravitational interactions along with strong, weak and electro-magnetic interactions. There exists theoretical models [19–23] which include spontaneous Lorentz invariance violation (LIV) and CPT violations in that more complete framework at Planck scale. At the observable low energy, these violations can give rise to minimal extension of SM through perturbative terms suppressed by M_P . Particles and anti-particles have same mass and lifetime due to CPT invariance. Any observed difference between masses or lifetimes of particles and anti-particles would be a signal for CPT violation. The present upper limit on CPT violation from kaon system is $|m_{K^0} - m_{\bar{K}^0}|/m_K < 6 \times 10^{-18}$ [24]. Since, kaons are Bosons and the natural mass term appearing in the Lagrangian is mass squared term, the above constraints can be rewritten as $|m_{K^0}^2 - m_{\bar{K}^0}^2| < 0.25 \text{ eV}^2$. Current neutrino oscillation data provide the bounds $|\Delta_{21} - \bar{\Delta}_{21}| < 5.9 \times 10^{-5} \text{ eV}^2$ and

$|\Delta_{31} - \bar{\Delta}_{31}| < 1.1 \times 10^{-3} \text{ eV}^2$ [25]. If these differences are non-zero and they are manifestation of some kind of CPT violating effects, they can induce changes in neutrino oscillation probabilities [26–29]. Various studies have been done about the LIV/CPT violation with neutrinos [30–45]. Several neutrino oscillation experiments have looked for LIV/CPT violations and put on constraints on the LIV/CPT violating parameters [46–53]. Ref. [54] includes the list of constraints on all the relevant LIV/CPT violating parameters. But till date no study has been made to look for LIV/CPT violation in the long baseline accelerator neutrino oscillation experiments **data**. In this paper, we will consider the minimal extension of SM that violates Lorentz invariance as well as CPT symmetry. We will test the model with the latest data from NO ν A and T2K and try to see if there is any hint of CPT violating LIV in the individual as well as combined data set and whether the tension between the two experiments can be resolved with the help of this new physics hypothesis.

In section II, we will discuss the theoretical framework of LIV in neutrino oscillation and present the comparison between oscillation probabilities with and without LIV. In section III, we will discuss the details method of our analysis and in section IV we will present our results after analysing data from NO ν A and T2K. The conclusion will be drawn in section V.

II. THEORETICAL FRAMEWORK

The Lorentz invariance violating neutrinos and anti-neutrinos can be described by the effective Lagrangian [26, 55]

$$\mathcal{L} = \bar{\Psi}_A \left(i\gamma_\mu \partial_\mu \delta_{AB} - M_{AB} + \hat{\mathcal{Q}}_{AB} \right) \Psi_B + \text{h.c.} \quad (\text{II.2})$$

$\Psi_{A(B)}$ is a $2N$ dimensional spinor containing $\psi_{\alpha(\beta)}$, which is a spinor field with $\alpha(\beta)$ ranging over N spinor flavours, and their charge conjugates given by $\psi_{\alpha(\beta)}^C = C\bar{\psi}_{\alpha(\beta)}^T$. Therefore, $\Psi_{A(B)}$ can be expressed as

$$\Psi_{A(B)} = \left(\psi_{\alpha(\beta)}, \psi_{\alpha(\beta)}^C \right)^T. \quad (\text{II.3})$$

$\hat{\mathcal{Q}}$ in eq. II.2 is a generic Lorentz invariance violating operator. The first term in the right side of eq. II.2 is the kinetic term, the second term is the mass term involving the mass matrix M and the third term gives rise to the LIV effect. $\hat{\mathcal{Q}}$ is small and perturbative in nature.

We will restrict ourselves only to the renormalizable Dirac couplings in the theory, i.e. terms only with mass dimension ≤ 4 will be incorporated. Doing so, one can write the Lorentz invariance violating Lagrangian in the flavour basis as [26]

$$\mathcal{L}_{\text{LIV}} = -\frac{1}{2} \left[a_{\alpha\beta}^{\mu} \bar{\psi}_{\alpha} \gamma_{\mu} \psi_{\beta} + b_{\alpha\beta}^{\mu} \bar{\psi}_{\alpha} \gamma_5 \gamma_{\mu} \psi_{\beta} - i c_{\alpha\beta}^{\mu\nu} \bar{\psi}_{\alpha} \gamma_{\mu} \partial_{\nu} \psi_{\beta} - i d_{\alpha\beta}^{\mu\nu} \bar{\psi}_{\alpha} \gamma_{\mu} \gamma_5 \partial_{\nu} \psi_{\beta} \right], \quad (\text{II.4})$$

where $a_{\alpha\beta}^{\mu}$, $b_{\alpha\beta}^{\mu}$, $c_{\alpha\beta}^{\mu\nu}$ and $d_{\alpha\beta}^{\mu\nu}$ Lorentz invariance violating parameters. Since, only left handed neutrinos are present in SM, the observable effects in the neutrino oscillation experiments can be parameterized as

$$(a_L)_{\alpha\beta}^{\mu} = (a + b)_{\alpha\beta}^{\mu}, (c_L)_{\alpha\beta}^{\mu\nu} = (c + d)_{\alpha\beta}^{\mu\nu}. \quad (\text{II.5})$$

These are constant Hermitian matrices which can modify the standard Hamiltonian in vacuum. The first combination involves CPT violation, where as the second combination is the CPT conserving Lorentz invariance violating neutrinos. In this paper, we will consider only direction independent isotropic terms, and hence we will only consider the $\mu = \nu = 0$. From now on, for simplicity, we will call $a_{\alpha\beta}^0$ terms as $a_{\alpha\beta}$ and $c_{\alpha\beta}^{00}$ term as $c_{\alpha\beta}$. Taking into account only these isotropic LIV terms, the neutrino Hamiltonian with LIV effect becomes:

$$H = H_{\text{vac}} + H_{\text{mat}} + H_{\text{LIV}}, \quad (\text{II.6})$$

where

$$H_{\text{vac}} = \frac{1}{2E} U \begin{bmatrix} m_1^2 & 0 & 0 \\ 0 & m_2^2 & 0 \\ 0 & 0 & m_3^2 \end{bmatrix} U^{\dagger}; H_{\text{mat}} = \sqrt{2} G_F N_e \begin{bmatrix} 1 & 0 & 0 \\ 0 & 0 & 0 \\ 0 & 0 & 0 \end{bmatrix}; \quad (\text{II.7})$$

$$H_{\text{LIV}} = \begin{bmatrix} a_{ee} & a_{e\mu} & a_{e\tau} \\ a_{e\mu}^* & a_{\mu\mu} & a_{\mu\tau} \\ a_{e\tau}^* & a_{\mu\tau}^* & a_{\tau\tau} \end{bmatrix} - \frac{4}{3} E \begin{bmatrix} c_{ee} & c_{e\mu} & c_{e\tau} \\ c_{e\mu}^* & c_{\mu\mu} & c_{\mu\tau} \\ c_{e\tau}^* & c_{\mu\tau}^* & c_{\tau\tau} \end{bmatrix}. \quad (\text{II.8})$$

G_F is the Fermi coupling constant and N_e is the electron density along the neutrino path. The $-4/3$ in front of the second term arises due to non observability of the Minkowski trace of the CPT conserving LIV term c_L which relates xx , yy , and zz component to the 00 component [26]. The effects of $a_{\alpha\beta}$ are proportional to the baseline L and those of $c_{\alpha\beta}$ are proportional to LE . In this paper, we will consider the effects of CPT violating LIV parameters $a_{\alpha\beta}$ only.

It is noteworthy that the Hamiltonian due to LIV is analogous to that with neutral current (NC) non standard interaction (NSI) during the propagation of neutrinos through matter

$$H' = H_{\text{vac}} + H_{\text{mat}} + H_{\text{NSI}}, \quad (\text{II.9})$$

where

$$H_{\text{NSI}} = \sqrt{2}G_F N_e \begin{bmatrix} \epsilon_{ee} & \epsilon_{e\mu} & \epsilon_{e\tau} \\ \epsilon_{e\mu}^* & \epsilon_{\mu\mu} & \epsilon_{\mu\tau} \\ \epsilon_{e\tau}^* & \epsilon_{\mu\tau}^* & \epsilon_{\tau\tau} \end{bmatrix}. \quad (\text{II.10})$$

$\epsilon_{\alpha\beta}$ are the strength of NSI. Thus, a relation between CPT violating LIV and NSI can be found by following equation [56]:

$$\epsilon_{\alpha\beta} = \frac{a_{\alpha\beta}}{\sqrt{2}G_F N_e}. \quad (\text{II.11})$$

In this work, we will consider the effects of parameters $a_{e\mu} = |a_{e\mu}|e^{i\phi_{e\mu}}$ and $a_{e\tau} = |a_{e\tau}|e^{i\phi_{e\tau}}$, because these two parameters have the highest influences on $\nu_\mu \rightarrow \nu_e$ oscillation probability [45], which is responsible for octant, δ_{CP} , and hierarchy sensitivity of long baseline accelerator neutrino like NO ν A and T2K. Since, we are mostly concerned about determining these unknown standard oscillation parameters in the long baseline accelerator neutrino experiment, we fixed all other LIV parameters, except $a_{e\mu}$ and $a_{e\tau}$, to zero. It implies that in this paper, the contribution from Lorez invariance violation in the NO ν A and T2K experiments is coming only from the CPT violating Lorentz violation and mostly in the appearance channels. The ν_μ and $\bar{\nu}_\mu$ disappearance channels still conserve Lorentz invariance. The current constraint on these parameters from Super-kamiokande experiment at 95% confidence level (C.L.) is [51]

$$|a_{e\mu}| < 2.5 \times 10^{-23} \text{ GeV}; |a_{e\tau}| < 5 \times 10^{-23} \text{ GeV} \quad (\text{II.12})$$

The $\nu_\mu \rightarrow \nu_e$ oscillation probability in presence of LIV parameters $a_{e\mu}$ and $a_{e\tau}$ can be written in the similar way as the oscillation probability in presence of NSI parameters $\epsilon_{e\mu}$ and $\epsilon_{e\tau}$ [57–59]:

$$P_{\mu e}^{\text{SM+LIV}} \simeq P_{\mu e}(\text{SM}) + P_{\mu e}(a_{e\mu}) + P_{\mu e}(a_{e\tau}). \quad (\text{II.13})$$

The first term in eq. II.13 is the oscillation probability in the presence of standard matter

effect. It can be written as [60]

$$\begin{aligned}
P_{\mu e}(\text{SM}) &= \sin^2 2\theta_{13} \sin^2 \theta_{23} \frac{\sin^2 \hat{\Delta}(1 - \hat{A})}{(1 - \hat{A})^2} \\
&+ \alpha \cos \theta_{13} \sin 2\theta_{12} \sin 2\theta_{13} \sin 2\theta_{23} \cos(\hat{\Delta} + \delta_{CP}) \\
&\quad \frac{\sin \hat{\Delta} \hat{A} \sin \hat{\Delta}(1 - \hat{A})}{\hat{A} \quad 1 - \hat{A}} \\
&+ \alpha^2 \sin^2 2\theta_{12} \cos^2 \theta_{13} \cos^2 \theta_{23} \frac{\sin^2 \hat{\Delta} \hat{A}}{\hat{A}^2},
\end{aligned} \tag{II.14}$$

where $\alpha = \frac{\Delta_{21}}{\Delta_{31}}$, $\hat{\Delta} = \frac{\Delta_{31}L}{4E}$ and $\hat{A} = \frac{A}{\Delta_{31}}$. A is the Wolfenstein matter term [61], given by $A = 2\sqrt{2}G_F N_e E$, where E is the neutrino beam energy and L is the length of the baseline.

For the second and third terms in eq. II.13, describing the effects of $a_{e\mu}$ and $a_{e\tau}$ respectively, we follow the similar approach of NSI, described in references [57–59], and replace $\epsilon_{\alpha\beta}$ terms by $a_{\alpha\beta}$ terms according to eq. II.11. Doing so, we can write

$$\begin{aligned}
P_{\mu e}(a_{e\beta}) &= \frac{4|a_{e\beta}|\hat{A}\hat{\Delta} \sin \theta_{13} \sin 2\theta_{23} \sin \hat{\Delta}}{\sqrt{2}G_F N_e} [Z_{e\beta} \sin(\delta_{CP} + \phi_{e\beta}) + W_{e\beta} \cos(\delta_{CP} + \phi_{e\beta})] \\
&= \frac{4|a_{e\beta}|L \sin \theta_{13} \sin 2\theta_{23} \sin \hat{\Delta}}{2} [Z_{e\beta} \sin(\delta_{CP} + \phi_{e\beta}) + W_{e\beta} \cos(\delta_{CP} + \phi_{e\beta})]
\end{aligned} \tag{II.15}$$

where $\beta = \mu, \tau$;

$$\begin{aligned}
Z_{e\beta} &= -\cos \theta_{23} \sin \hat{\Delta}, \text{ if } \beta = \mu \\
&= \sin \theta_{23} \sin \hat{\Delta}, \text{ if } \beta = \tau
\end{aligned} \tag{II.16}$$

and

$$\begin{aligned}
W_{e\beta} &= \cos \theta_{23} \left(\frac{\sin^2 \theta_{23} \sin \hat{\Delta}}{\cos^2 \theta_{12} \hat{\Delta}} + \cos \hat{\Delta} \right), \text{ if } \beta = \mu \\
&= \sin \theta_{23} \left(\frac{\sin \hat{\Delta}}{\hat{\Delta}} - \cos \hat{\Delta} \right), \text{ if } \beta = \tau.
\end{aligned} \tag{II.17}$$

From, eq. II.15, it can be seen that the LIV effects considered in this paper are matter independent.

The oscillation probability $P_{\bar{\mu}\bar{e}}$ for anti-neutrino can be calculated from equations II.14 and II.15 by substituting $A \rightarrow -A$, $\delta_{CP} \rightarrow -\delta_{CP}$, $|a_{e\beta}| \rightarrow -|a_{e\beta}|$ and $\phi_{e\beta} \rightarrow -\phi_{e\beta}$, where $\beta = \mu, \tau$.

In our analysis, however, we have used GLOBES [62, 63] to calculate the oscillation probability. To do so, we modified the probability code of the software to include LIV. After that, GLOBES is capable of calculating the oscillation probability without the approximations required to derive equations II.13-II.15. The evolution equation for a neutrino state $|\nu\rangle = (|\nu_e\rangle, |\nu_\mu\rangle, |\nu_\tau\rangle)^T$ travelling a small distance x can be written in presence of LIV as

$$i\frac{d}{dx}|\nu\rangle = H|\nu\rangle. \quad (\text{II.18})$$

H is the Hamiltonian from eq. II.6. The oscillation probability of $\nu_\mu \rightarrow \nu_e$ after travelling through a distance L can be written as

$$P_{\mu e}^{\text{SM+LIV}} = |\langle \nu_e | e^{-iHL} | \nu_\mu \rangle|^2. \quad (\text{II.19})$$

In fig. 1, we have shown the effects of $|a_{e\mu}|$ and $|a_{e\tau}|$ on the oscillation probability for NH of NO ν A for different values of δ_{CP} and $\phi_{e\mu}$, $\phi_{e\tau}$. To generate these plots, we have fixed the standard oscillation parameter values to their best-fit values taken from [7, 8]. It is obvious that there is a large difference between standard oscillation and oscillation with LIV at probability level. This difference makes our motivation to test LIV with oscillation data from long baseline experiments even stronger. It can be observed that $\phi_{e\mu}$ ($\phi_{e\tau}$) have quite opposite effects on $P_{\mu e}$ compared to that of δ_{CP} .

In fig. 2, we have shown the similar comparison for T2K. It is obvious that the effect of LIV is less prominent in case of T2K than it was for NO ν A. It is expected because the CPT violating LIV effect is proportional to the length of the baseline and T2K baseline (295 km) is very small compared to that of NO ν A (810 km).

It would be interesting to note down the the ability to discriminate between the two models for different δ_{CP} values and baselines. To do so, we first fixed the neutrino energy at the NO ν A flux peak enegy 2.0 GeV and varied δ_{CP} in the range $[-180^\circ : 180^\circ]$ and the baseline from 100 km to 1400 km. In figures 3-5, the ratio between $P_{\mu e}^{\text{SM+LIV}}$ and $P_{\mu e}^{\text{SM}}$ has been shown as a function of L/E and δ_{CP} for different $\phi_{e\mu}$ and $\phi_{e\tau}$. values mentioned in the figure panels. $|a_{e\mu}|$ and $|a_{e\tau}|$ have been fixed at 2×10^{-23} GeV each. The standard oscillation parameters have been fixed at the current global best-fit values taken from [7, 8]. The farther away the ratio is from 1, the better is the discrimination capability between the two models. It can be said that with 810 km baseline and flux peak energy at 2.0 GeV, NO ν A has a

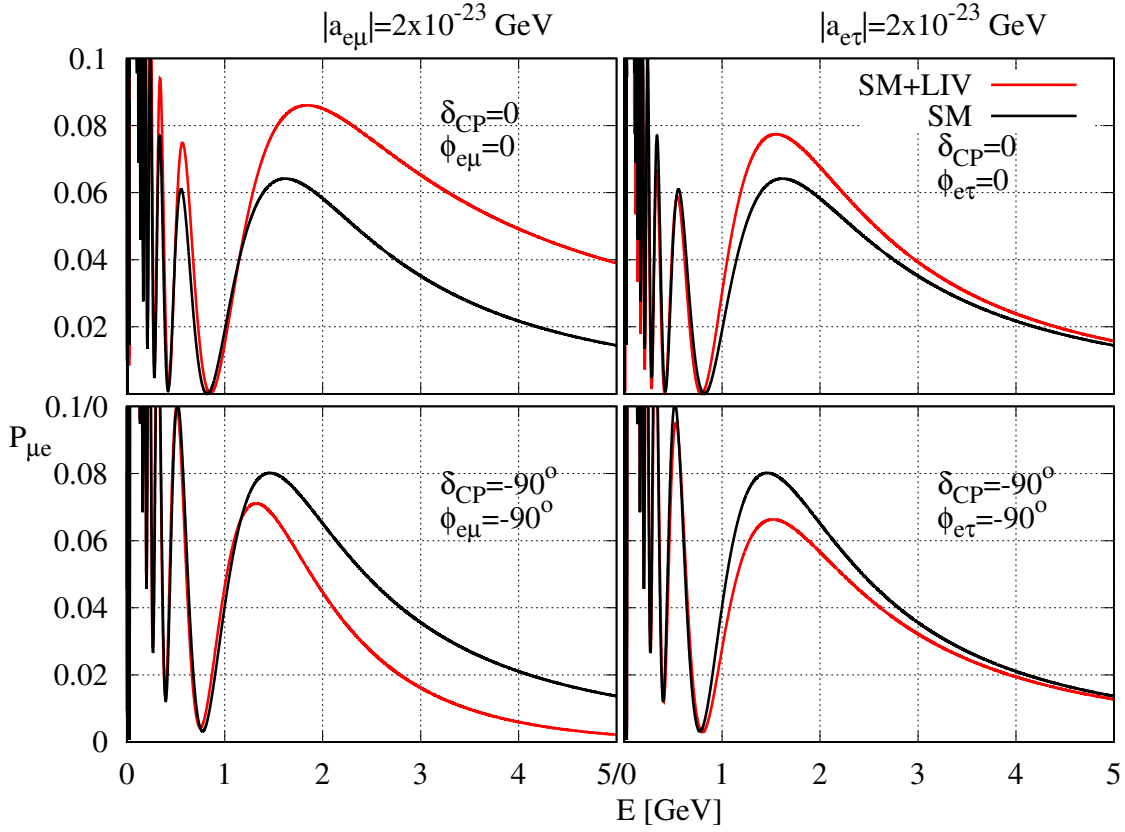


FIG. 1: Effect of $|a_{e\mu}|(|a_{e\tau}) = 2 \times 10^{-23}$ GeV on the oscillation probability for NH of $\text{NO}\nu\text{A}$ in the left (right panel). The black line shows the oscillation probability with standard matter effect. The standard oscillation parameter values have been fixed to their best-fit values [7, 8]. The red line indicates the oscillation probability with LIV effect. Values of δ_{CP} , $\phi_{e\mu}$ and $\phi_{e\tau}$ have been mentioned in the panels.

good discrimination capability between the two models at the oscillation probability level for all three cases and with both the hierarchies.

In the next step, we repeated the same exercise by fixing the energy $E = 0.7$ GeV at the T2K flux peak energy. The results have been shown in figures 6-8. It can be observed that T2K with its baseline of $L = 295$ km, has a good discrimination capability at the probability level between the two models for most of the CP violating δ_{CP} values except for ν ($\bar{\nu}$) run when the hierarchy is IH (NH) and $\phi_{e\mu} = \phi_{e\tau} = 0$.

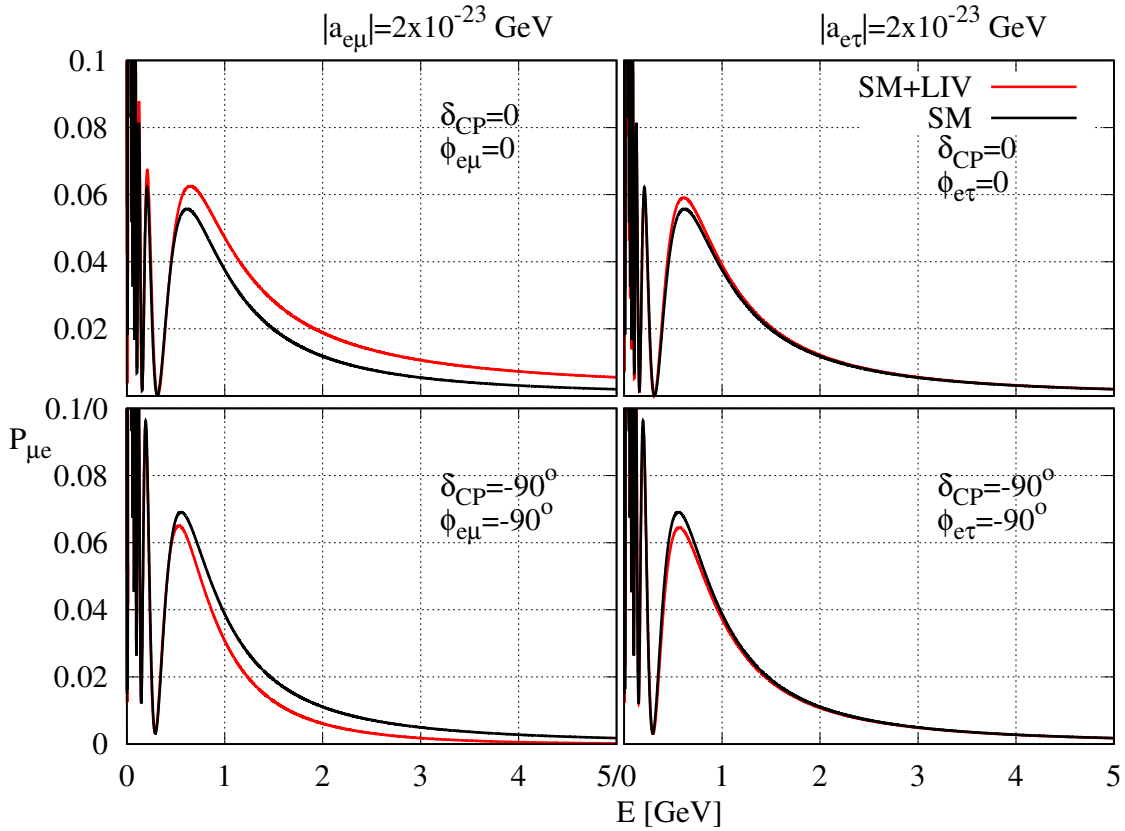


FIG. 2: Effect of $|a_{e\mu}|(|a_{e\tau}) = 2 \times 10^{-23}$ GeV on the oscillation probability for NH of T2K in the left (right panel). The black line shows the oscillation probability with standard matter effect. The standard oscillation parameter values have been fixed to their best-fit values [7, 8]. The red line indicates the oscillation probability with LIV effect. Values of δ_{CP} , $\phi_{e\mu}$ and $\phi_{e\tau}$ have been mentioned in the panels.

III. ANALYSIS DETAILS

The NO ν A detector [10] is a 14 kt totally active scintillator detector (TASD), placed 810 km away from the neutrino source at the Fermilab and it is situated at 0.8° off-axis of the NuMI beam. The flux peaks at 2 GeV, close to the oscillation maxima at 1.4 GeV for NH and at 1.8 GeV for IH. NO ν A started taking data in 2014 and took data that until 2020 release [12], correspond to 1.36×10^{21} (1.25×10^{21}) POT in ν ($\bar{\nu}$) mode. The T2K experiment [11] uses the ν_μ beam from the J-PARC accelerator at Tokai and the water Cherenkov detector at Super-Kamiokande, which is 295 km away from the source. The detector is situated 2.5° off-axis. The flux peaks at 0.7 GeV, which is also close to the first oscillation maximum. T2K started taking data in 2009 and until 2020 release of results these [13] correspond to

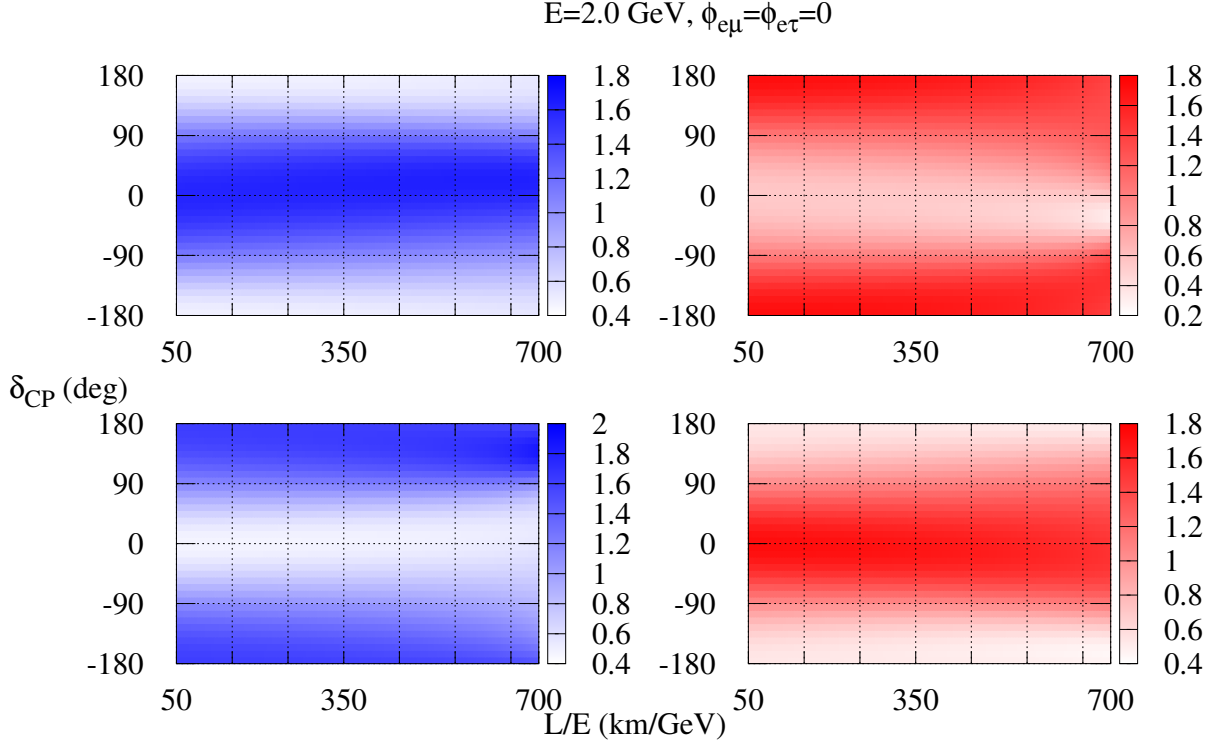


FIG. 3: Ratio of the LIV to standard oscillation probabilities as a function of L/E and δ_{CP} . The reference energy $E = 2.0$ GeV has been fixed to the $\text{NO}\nu\text{A}$ flux peak energy. For this peak energy and $\text{NO}\nu\text{A}$ baseline, $L/E = 405$ km/GeV. The upper (lower) panel shows the ratio for NH (IH), the left (right) panel shows it for neutrino (anti-neutrino). $|a_{e\mu}|$ and $|a_{e\tau}|$ have been fixed at 2×10^{-23} GeV each and we have set $\phi_{e\mu} = \phi_{e\tau} = 0$.

1.97×10^{21} (1.63×10^{21}) POT in ν ($\bar{\nu}$) mode.

To analyse the data, we kept $\sin^2 \theta_{12}$ and Δ_{21} to their best-fit values 0.304 and $7.42 \times 10^{-5} \text{ eV}^2$. These parameters have been determined by measuring electron neutrino survival probabilities in solar neutrino experiments. The LIV parameters which mostly affect electron neutrino survival probabilities are a_{ee} . We have fixed this parameter to zero. Therefore, the new physics should not affect the results from the solar neutrino experiments. We varied $\sin^2 2\theta_{13}$ in its 3σ range around its central value 0.084 with 3.5% uncertainty. $\sin^2 \theta_{23}$ has been varied in its 3σ range [0.41 : 0.62]. These ranges have been taken from the global best-fit ranges given in ref. [64]. These global fit was done without the 2020 data from $\text{NO}\nu\text{A}$ and

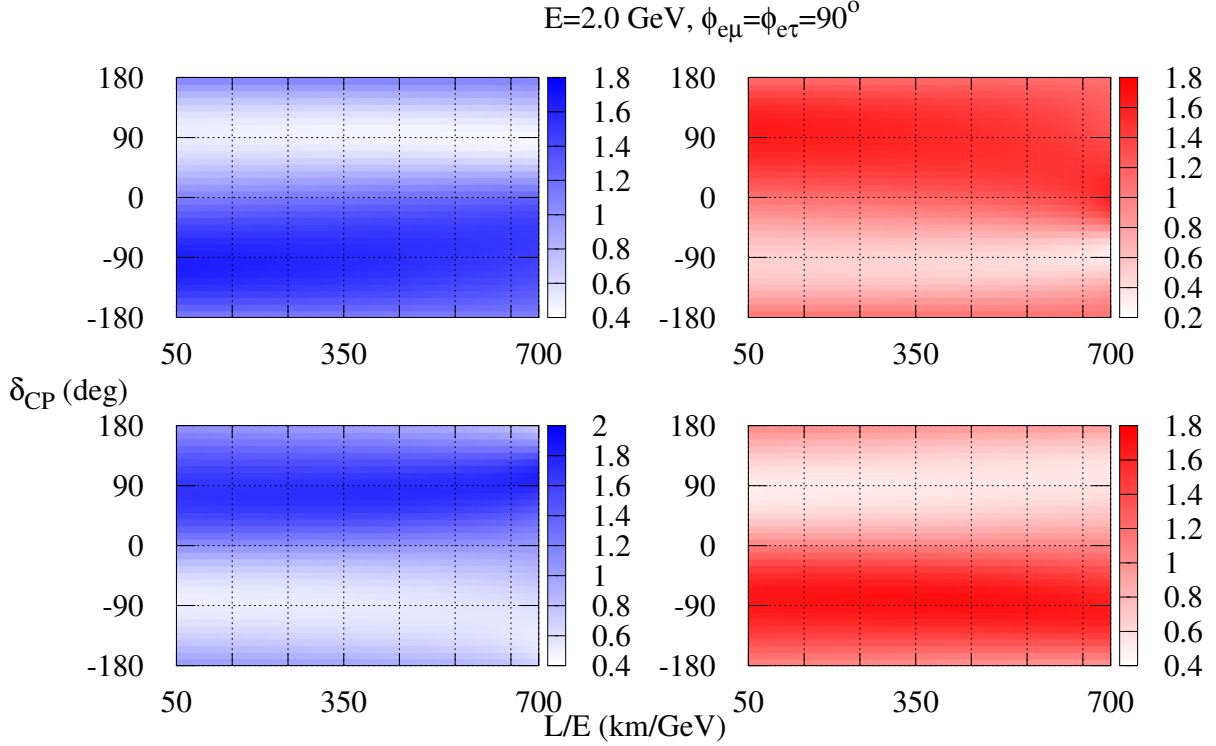


FIG. 4: Ratio of the LIV to standard oscillation probabilities as a function of L/E and δ_{CP} . The reference energy $E = 2.0$ GeV has been fixed to the $\text{NO}\nu A$ flux peak energy. For this peak energy and $\text{NO}\nu A$ baseline, $L/E = 405$ km/GeV. The upper (lower) panel shows the ratio for NH (IH), the left (right) panel shows it for neutrino (anti-neutrino). $|a_{e\mu}|$ and $|a_{e\tau}|$ have been fixed at 2×10^{-23} GeV each and we have set $\phi_{e\mu} = \phi_{e\tau} = 90^\circ$.

T2K. We varied $|\Delta_{\mu\mu}|$ in its 3σ range around the MINOS best-fit value $2.32 \times 10^{-3} \text{ eV}^2$ with 3% uncertainty [65]. $\Delta_{\mu\mu}$ is related with Δ_{31} by the following relation [66]

$$\Delta_{\mu\mu} = \sin^2 \theta_{23} \Delta_{31} + \cos^2 \theta_{12} \Delta_{32} + \cos \delta_{CP} \sin 2\theta_{12} \sin \theta_{13} \tan \theta_{12} \Delta_{21}. \quad (\text{III.20})$$

The CP violating phase δ_{CP} has been varied in its complete range $[-180^\circ : 180^\circ]$.

Among the new physics parameters, $|a_{e\mu}|$ and $|a_{e\tau}|$ have been varied in the range $0 - 20 \times 10^{-23}$ GeV range. The phases $\phi_{e\mu}$ and $\phi_{e\tau}$ have been varied in the range $[-180^\circ : 180^\circ]$.

We calculated the theoretical event rates and the χ^2 between data and theoretical event rates using GLOBES [62, 63]. The data has been taken from [12, 13]. To calculate the theoretical event rates, we fixed the signal and background efficiencies by matching with

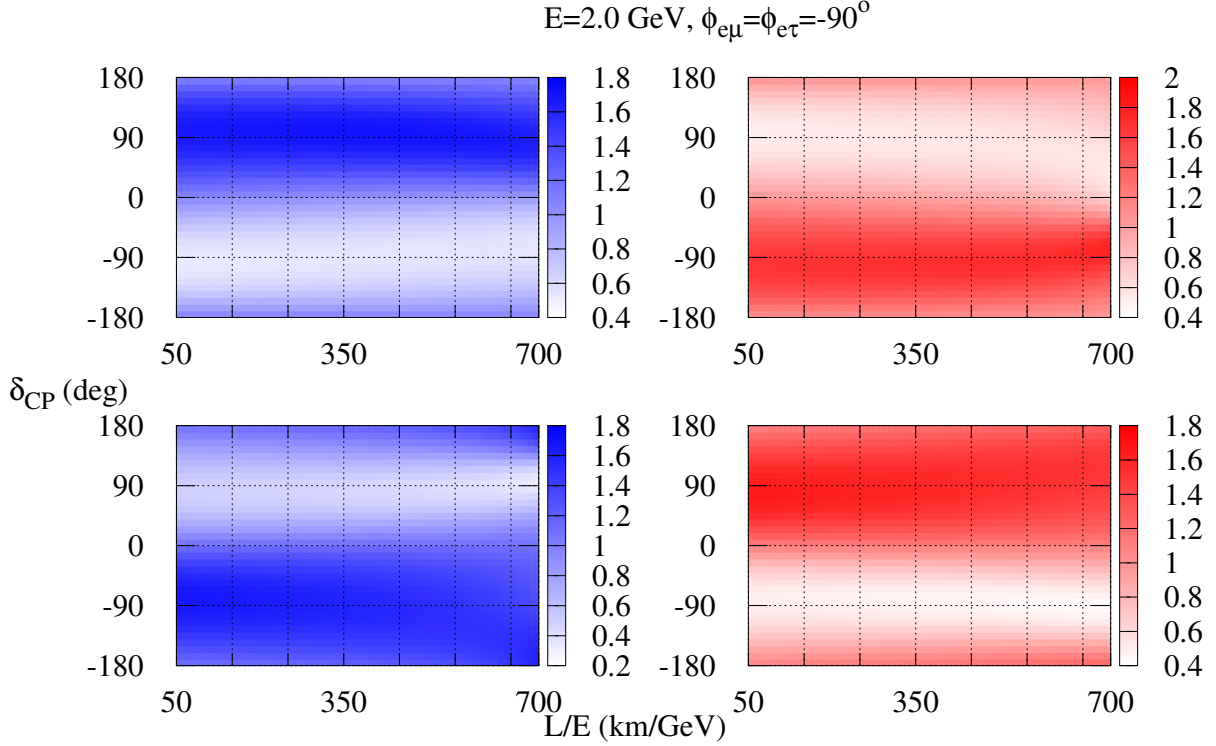


FIG. 5: Ratio of the LIV to standard oscillation probabilities as a function of L/E and δ_{CP} . The reference energy $E = 2.0$ GeV has been fixed to the $\text{NO}\nu\text{A}$ flux peak energy. For this peak energy and $\text{NO}\nu\text{A}$ baseline, $L/E = 405$ km/GeV. The upper (lower) panel shows the ratio for NH (IH), the left (right) panel shows it for neutrino (anti-neutrino). $|a_{e\mu}|$ and $|a_{e\tau}|$ have been fixed at 2×10^{-23} GeV each and we have set $\phi_{e\mu} = \phi_{e\tau} = -90^\circ$.

the Monte-Carlo simulations given by the collaborations [12, 13]. Automatic bin based energy smearing for generated theoretical events has been implemented in the same way as described in the GLOBES manual [62, 63]. For this purpose, we used a Gaussian smearing function

$$R^c(E, E') = \frac{1}{\sqrt{2\pi}} e^{-\frac{(E-E')^2}{2\sigma^2(E)}}, \quad (\text{III.21})$$

where E' is the reconstructed energy. The energy resolution function is given by

$$\sigma(E) = \alpha E + \beta\sqrt{E} + \gamma. \quad (\text{III.22})$$

For $\text{NO}\nu\text{A}$, we used $\alpha = 0.11$ (0.09), $\beta = \gamma = 0$ for electron (muon) like events. For T2K, we used $\alpha = 0$, $\beta = 0.075$, $\gamma = 0.05$ for both electron and muon like events.

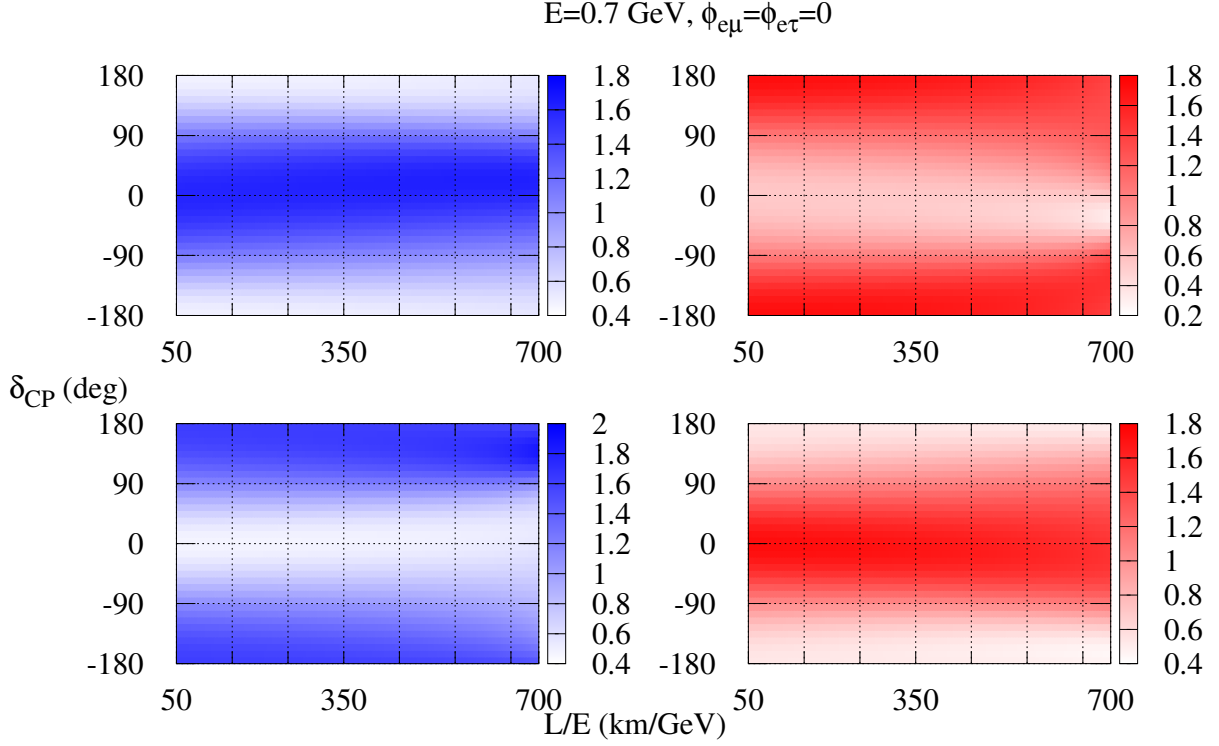


FIG. 6: Ratio of the LIV to standard oscillation probabilities as a function of L/E and δ_{CP} . The reference energy $E = 0.7 \text{ GeV}$ has been fixed to the T2K flux peak energy. For this peak energy and T2K baseline, $L/E = 421 \text{ km/GeV}$. The upper (lower) panel shows the ratio for NH (IH), the left (right) panel shows it for neutrino (anti-neutrino). $|a_{e\mu}|$ and $|a_{e\tau}|$ have been fixed at $2 \times 10^{-23} \text{ GeV}$ each and we have

$$\text{set } \phi_{e\mu} = \phi_{e\tau} = 0.$$

For $\text{NO}\nu\text{A}$, we used

- 5% normalisation and 5% energy calibration systematics uncertainty for e like events, and
- 5% normalisation and 0.01% energy calibration systematics uncertainty for μ like events.

For T2K, we used

- 5% normalisation and 5% energy calibration systematics uncertainty for e like events, and

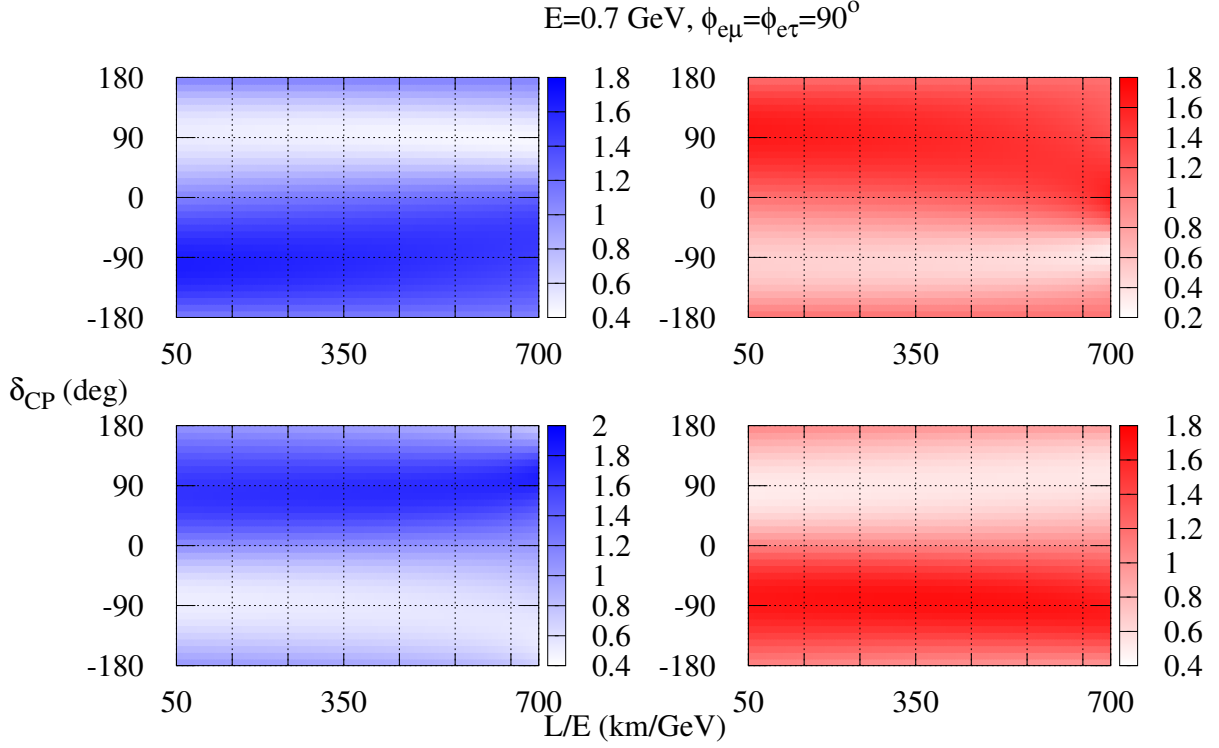


FIG. 7: Ratio of the LIV to standard oscillation probabilities as a function of L/E and δ_{CP} . The reference energy $E = 0.7 \text{ GeV}$ has been fixed to the T2K flux peak energy. For this peak energy and T2K baseline, $L/E = 421 \text{ km/GeV}$. The upper (lower) panel shows the ratio for NH (IH), the left (right) panel shows it for neutrino (anti-neutrino). $|a_{e\mu}|$ and $|a_{e\tau}|$ have been fixed at $2 \times 10^{-23} \text{ GeV}$ each and we have

$$\text{set } \phi_{e\mu} = \phi_{e\tau} = 90^\circ.$$

- 5% normalisation and 0.01% energy callibration systematics uncertainty for μ like events.

Implementing systematics uncertainty has been discussed in details in GLOBES manual [62, 63]. During the calculations of χ^2 we added priors on $\sin^2 2\theta_{13}$. After calculating χ^2 , we found out minimum of these χ^2 s and subtracted it from all the χ^2 s to calculate $\Delta\chi^2$.

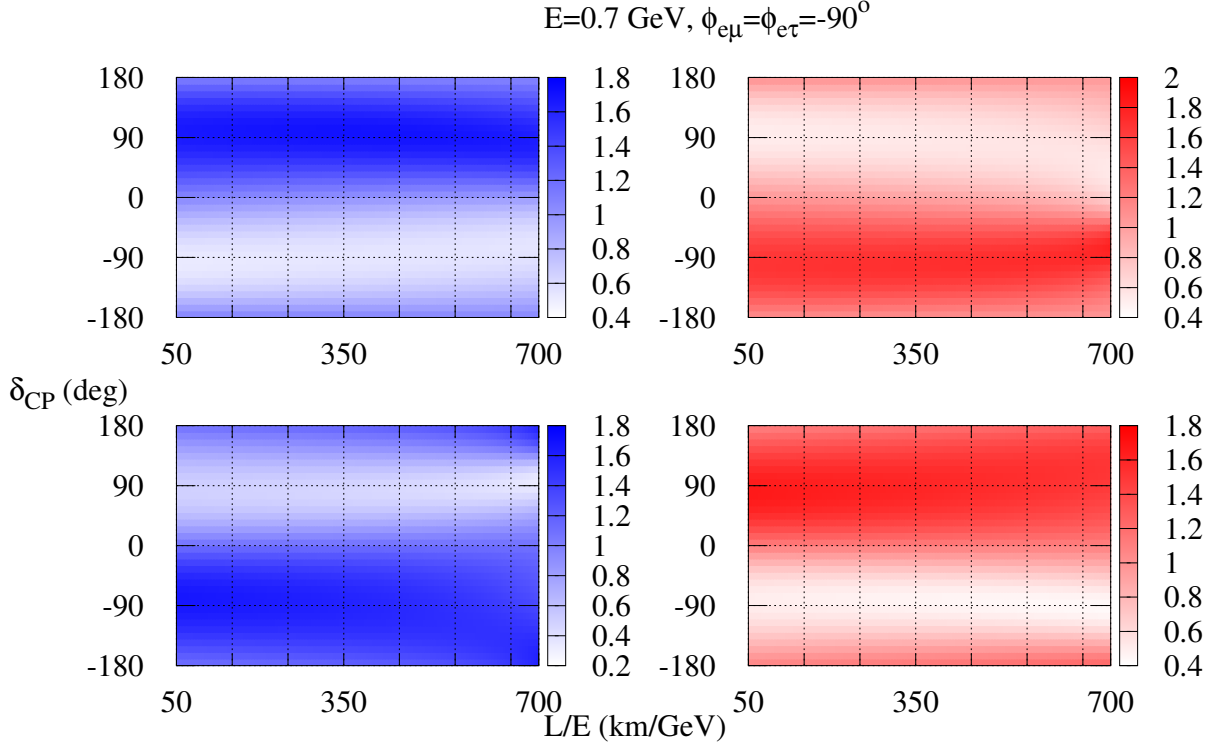


FIG. 8: Ratio of the LIV to standard oscillation probabilities as a function of L/E and δ_{CP} . The reference energy $E = 0.7 \text{ GeV}$ has been fixed to the T2K flux peak energy. For this peak energy and T2K baseline, $L/E = 421 \text{ km/GeV}$. The upper (lower) panel shows the ratio for NH (IH), the left (right) panel shows it for neutrino (anti-neutrino). $|a_{e\mu}|$ and $|a_{e\tau}|$ have been fixed at $2 \times 10^{-23} \text{ GeV}$ each and we have

$$\text{set } \phi_{e\mu} = \phi_{e\tau} = -90^\circ.$$

IV. RESULTS AND DISCUSSIONS

At first, we have analysed the data with the standard matter effect without any LIV hypothesis. The minimum χ^2 for $\text{NO}\nu\text{A}$ (T2K) with 50 (88) bins is 48.65 (95.85) and it is at NH. For the combined analysis, the minimum χ^2 with 138 bins is 147.14 and it occurs at IH. In fig. 9, we have shown the analysis in the $\sin^2 \theta_{23} - \delta_{CP}$ plane. This plot is comparable to the ones presented by the collaborations in references [12, 13]. It is evident that there is a tension between the two experiments in terms of the best-fit δ_{CP} values. Moreover, there is no overlap between the 1σ region of each experiment.

Once the standard analysis is done, we proceeded to analyse the data with LIV hypothesis.

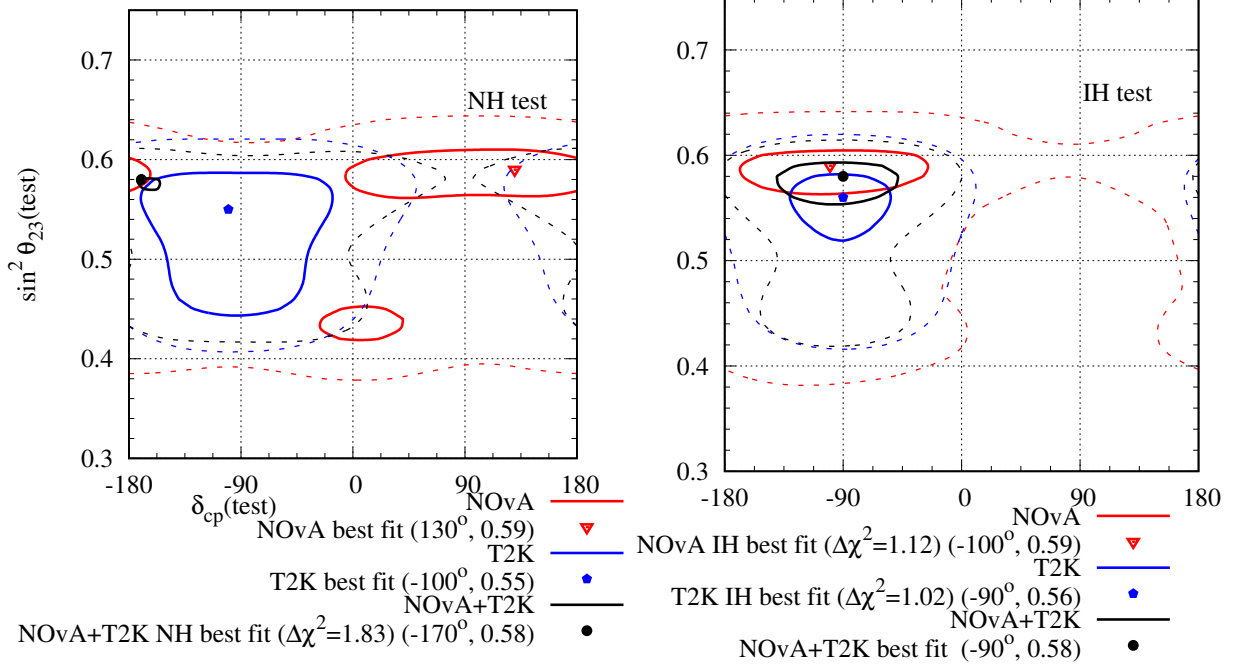


FIG. 9: Allowed region in the $\sin^2 \theta_{23} - \delta_{CP}$ plane after analysing NO ν A and T2K complete data set with standard matter effect without LIV hypothesis. The left (right) panel represents test hierarchy NH (IH). The red (blue) lines indicate the results for NO ν A (T2K) and the black line indicates the combined analysis of both. The solid (dashed) lines indicate the 1σ (3σ) allowed regions. The minimum χ^2 for NO ν A (T2K) with 50 (88) bins is 48.65 (95.85) and it occurs at NH. For the combined analysis, the minimum χ^2 with 138 bins is 147.14.

We found out that the minimum χ^2 for NO ν A (T2K) with 50 (88) bins is 47.71 (93.14) and it is at NH. Both the experiments, however, have a degenerate solution at IH with $\Delta\chi^2 = 0.1$. For the combined analysis the minimum χ^2 is 145.09 at IH for 138 bins. The combined analysis has a degenerate solution at NH with $\Delta\chi^2 = 0.1$. Therefore, the present accelerator neutrino oscillation data has no hierarchy sensitivity when analysed with LIV.

In fig. 10, we have presented our result with LIV hypothesis on the $\sin^2 \theta_{23} - \delta_{CP}$ plane. T2K (NO ν A) disfavours (includes) NO ν A (T2K) best-fit points at 1σ C.L. Now, there is a large overlap between the 1σ allowed regions of the two experiments. Hence, one can

conclude that the tension between the two experiments gets reduced when the data are analysed with LIV. However, there is a new mild tension in terms of the best-fit $\sin^2 \theta_{23}$ values. θ_{23} at T2K best-fit point is at lower octant, while the same is at higher octant for NO ν A. But NO ν A has a nearly degenerate ($\Delta\chi^2 = 0.35$) best-fit point at lower octant. Similarly, T2K also cannot rule out higher octant at 1σ C.L. Thus, both the experiments lose their octant sensitivity when analysed with LIV. In fig. 11, we have shown $\Delta\chi^2$ as

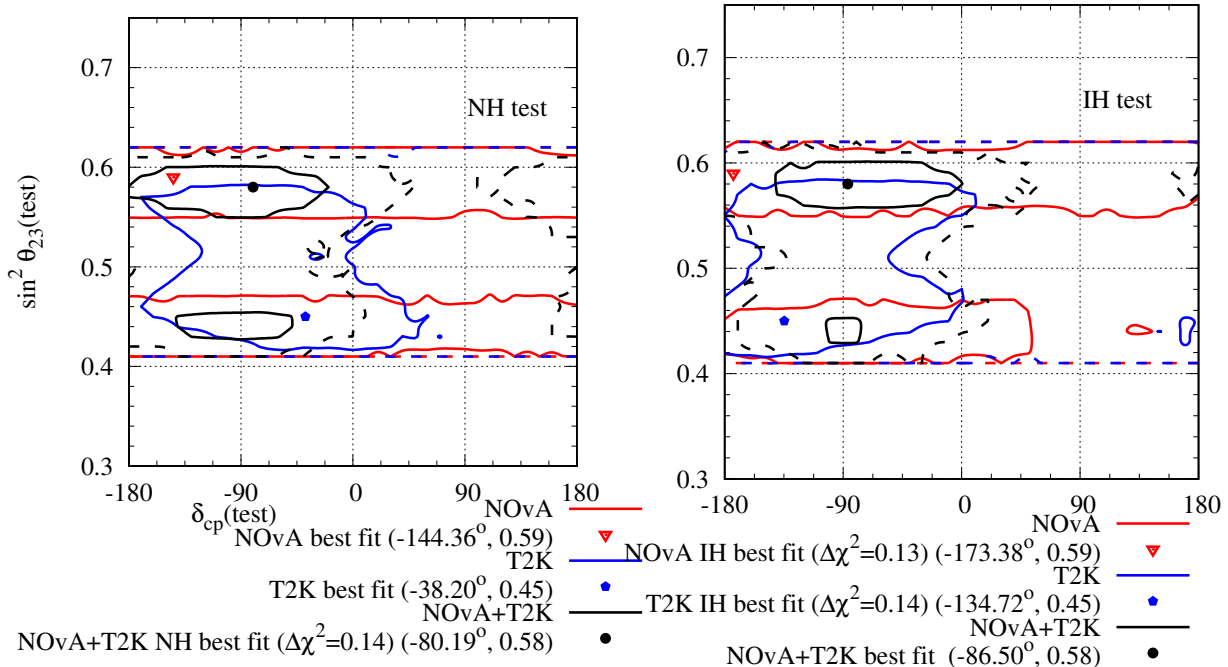


FIG. 10: Allowed region in the $\sin^2 \theta_{23} - \delta_{CP}$ plane after analysing NO ν A and T2K complete data set with LIV hypothesis. The left (right) panel represents test hierarchy NH (IH). The red (blue) lines indicate the results for NO ν A (T2K) and the black line indicates the combined analysis of both. The solid (dashed) lines indicate the 1σ (3σ) allowed regions. The minimum χ^2 for NO ν A (T2K) with 50 (88) bins is 47.71 (93.14) and it occurs at NH. For the combined analysis, the minimum χ^2 with 138 bins is 145.09.

a function of the individual LIV parameters. To do so, we marginalised $\Delta\chi^2$ on all the parameters except the one against which we want to plot it. It can be seen from fig. 11 that both $|a_{e\mu}| = 0$ and $|a_{e\tau}| = 0$ values have $\Delta\chi^2 > 1$ for T2K. For NO ν A however, both these

| Parameters | standard | | LIV | | 90% | |
|---|---------------------------|----------------------------|--|--|--------|---------|
| | NH | IH | NH | IH | NH | IH |
| $\frac{\Delta_{\mu\mu}}{10^{-3} eV^2}$ | $2.44^{+0.02}_{-0.048}$ | $-(2.44^{+0.02}_{-0.048})$ | $2.40^{+0.004}_{-0.026}$ | $-(2.41^{+0.01}_{-0.05})$ | | |
| $\sin^2 2\theta_{13}$ | $0.084^{+0.002}_{-0.002}$ | $0.084^{+0.003}_{-0.002}$ | $0.084^{+0.002}_{-0.003}$ | $0.084^{+0.002}_{-0.003}$ | | |
| $\sin^2 \theta_{23}$ | $0.59^{+0.01}_{-0.01}$ | $0.59^{+0.01}_{-0.02}$ | $0.43^{+0.03}_{-0.02} \oplus 0.59^{+0.03}_{-0.03}$ | $0.43^{+0.02}_{-0.01} \oplus 0.59^{+0.03}_{-0.03}$ | | |
| $\delta_{CP}/^\circ$ | 130^{+40}_{-110} | $-(100^{+50}_{-60})$ | -144.36 | -173.38 | | |
| $\frac{ a_{e\mu} }{10^{-23} \text{GeV}}$ | | | 4.81 | 2.22 | < 8.19 | < 7.78 |
| $\frac{ a_{e\tau} }{10^{-23} \text{GeV}}$ | | | 2.52 | $5.33^{+9.20}_{-5.33}$ | < 3.18 | < 15.71 |
| $\phi_{e\mu}$ | | | -114.52 | 141.18 | | |
| $\phi_{e\tau}/^\circ$ | | | -145.02 | 25.04 | | |

TABLE II: Parameter values at the best-fit points for NO ν A. The 1σ error bars have been mentioned where possible. The 90% limits for 1 d.o.f have also been mentioned.

values have $\Delta\chi^2 < 1$. For the combined analysis, $|a_{e\mu}| = 0$ has a $\Delta\chi^2 > 1$, but $|a_{e\tau}| = 0$ has $\Delta\chi^2 < 1$. Therefore, it can be said that the present NO ν A data do not favour any of the two hypotheses over the other. However T2K data and the combined analysis disfavour standard oscillation at 1σ C.L. In tables II, III and IV, we have presented the best-fit values of the standard and non-standard unknown oscillation parameters.

To emphasize our result, in fig. 12, we have presented the expected electron and positron events rates for each energy bins for both standard oscillation and oscillation with LIV as a function of energy for both NO ν A and T2K. The experimental event rates have also been plotted. It is obvious that for NO ν A, there is not any significant difference between the expected event rates at best-fit points of the two models and both models give a good fit to the data. However, for T2K, there is a clear distinction at the expected event rates at the best-fit points of the two models. Also, LIV gives a better fit to the data especially at energies close to the flux peak energy.

V. CONCLUSION

At present, NO ν A cannot disfavour any of the two hypotheses. However, both T2K and the combined analysis disfavours standard oscillation at 1σ C.L. The latest accelerator

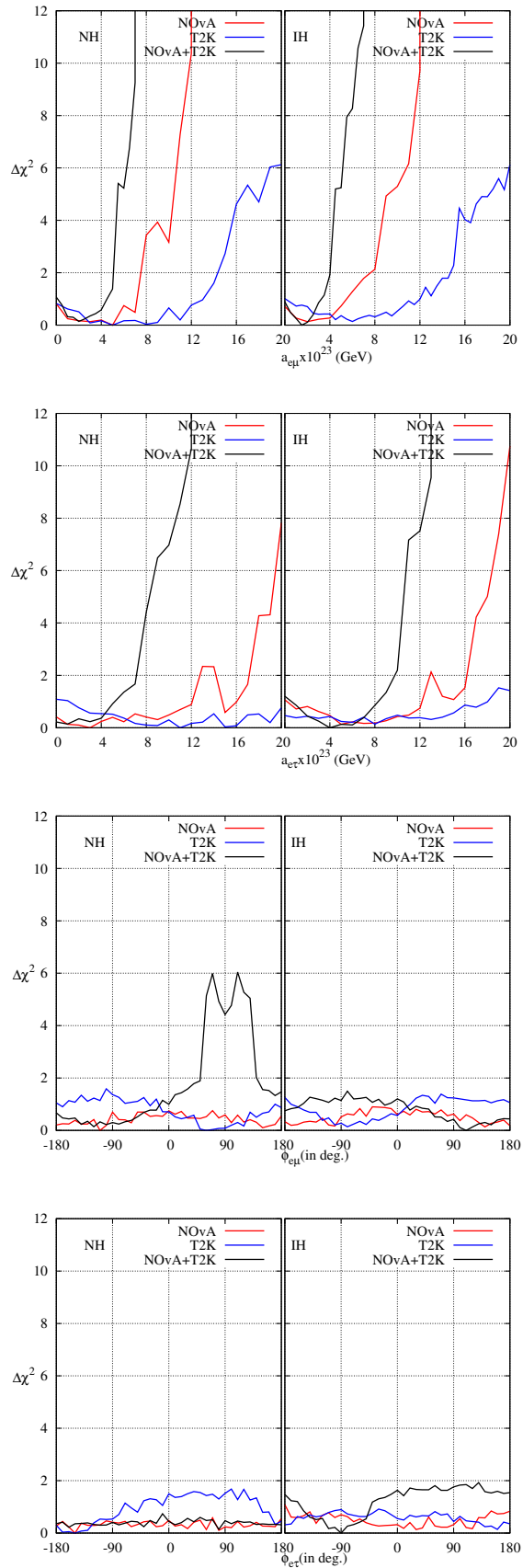


FIG. 11: $\Delta\chi^2$ as a function of individual LIV parameters.

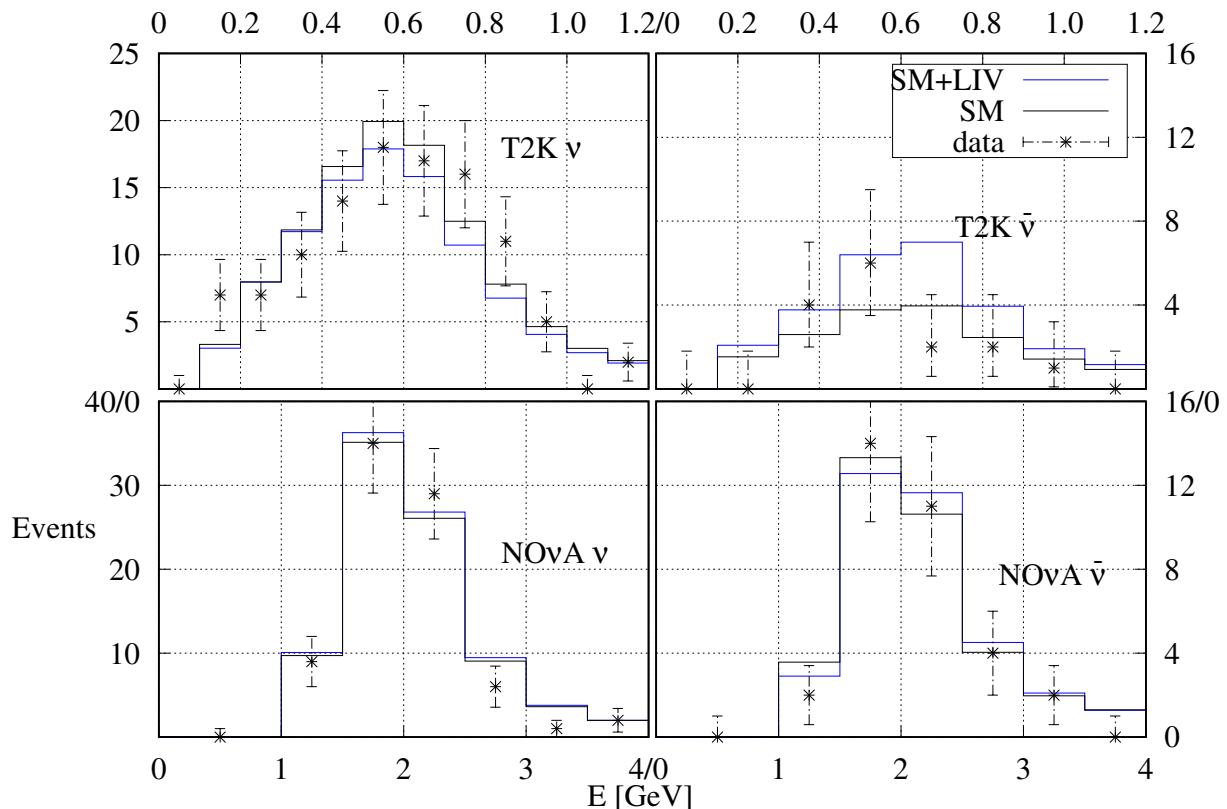


FIG. 12: Expected binned electron and positron event rates as a function of energy at the best-fit points for both the models and for both NO ν A and T2K experiments. The experimental event rates have also been plotted.

neutrino oscillation data lose hierarchy sensitivity when analysed with LIV. The 1σ allowed regions from the two experiments have a large overlap with LIV, unlike the standard oscillation case. Therefore, one can comment that the tension between the two experiments is reduced when the data are analysed with LIV. However, there is a new mild tension between the best-fit values of $\sin^2 \theta_{23}$. While θ_{23} for NO ν A best-fit is at HO, it is at LO for the T2K best-fit point. But NO ν A (T2K) has a nearly degenerate best-fit point at lower (higher) octant as well. Therefore, both NO ν A and T2K data do not have octant and hierarchy determination capability when analysed with LIV.

In light of these, we recommend that the long baseline accelerator neutrino experiments to be analysed with LIV along with other BSM physics. If the future data continue to favour LIV over standard oscillation, it can be considered as a prominent signal for LIV.

| Parameters | standard | | LIV | | 90% | |
|--|---------------------------|------------------------------|------------------------------|-------------------------------|--------------|--------------|
| | NH | IH | NH | IH | NH | IH |
| $\frac{\Delta_{\mu\mu}}{10^{-3}\text{eV}^2}$ | $2.512_{-0.048}^{+0.048}$ | $-(2.512_{+0.048}^{-0.048})$ | $2.462_{-0.04}^{+0.04}$ | $-(2.47_{-0.03}^{+0.05})$ | | |
| $\sin^2 2\theta_{13}$ | $0.084_{-0.002}^{+0.002}$ | $0.084_{-0.002}^{+0.003}$ | $0.084_{-0.003}^{+0.002}$ | $0.084_{-0.003}^{+0.002}$ | | |
| $\sin^2 \theta_{23}$ | $0.55_{-0.09}^{+0.03}$ | $0.56_{-0.03}^{+0.02}$ | $0.45_{-0.03}^{+0.03}$ | $0.45_{-0.03}^{+0.03}$ | | |
| $\delta_{CP}/^\circ$ | $-(100_{-60}^{+50})$ | $-(90_{-30}^{+30})$ | $-(38.20_{-66.04}^{+65.71})$ | $-(134.72_{-70.57}^{+45.28})$ | | |
| $\frac{ a_{e\mu} }{10^{-23}\text{GeV}}$ | | | 4.60 | $6.17_{-6.02}^{+4.86}$ | < 15.25 | < 14.92 |
| $\frac{ a_{e\tau} }{10^{-23}\text{GeV}}$ | | | 11.14 | 8.06 | Out of range | Out of range |
| $\phi_{e\mu}$ | | | 64.29 | -77.34 | | |
| $\phi_{e\tau}/^\circ$ | | | -153.24 | 158.07 | | |

TABLE III: Parameter values at the best-fit points for T2K. The 1σ error bars have been mentioned where possible. The 90% limits for 1 d.o.f have also been mentioned.

VI. ACKNOWLEDGEMENT

U.R. thanks Prof. Soebur Razzaque for the valuable comments.

-
- [1] J. N. Bahcall, M. C. Gonzalez-Garcia, and C. Pena-Garay, *JHEP* **08**, 016 (2004), hep-ph/0406294.
- [2] Q. R. Ahmad et al. (SNO), *Phys. Rev. Lett.* **89**, 011301 (2002), nucl-ex/0204008.
- [3] R. Nichol (MINOS) (2012), talk given at the Neutrino 2012 Conference, June 3-9, 2012, Kyoto, Japan, <http://neu2012.kek.jp/>.
- [4] F. An et al. (DAYA-BAY), *Phys.Rev.Lett.* **108**, 171803 (2012), 1203.1669.
- [5] J. Ahn et al. (RENO), *Phys.Rev.Lett.* **108**, 191802 (2012), 1204.0626.
- [6] Y. Abe et al. (Double Chooz), *Phys.Rev.Lett.* **108**, 131801 (2012), 1112.6353.
- [7] (????).
- [8] I. Esteban, M. C. Gonzalez-Garcia, M. Maltoni, T. Schwetz, and A. Zhou, *JHEP* **09**, 178 (2020), 2007.14792.

| Parameters | standard | | LIV | | 90% | |
|---|---------------------------|------------------------------|--|------------------------------|--------|--------|
| | NH | IH | NH | IH | NH | IH |
| $\frac{\Delta_{\mu\mu}}{10^{-3} \text{eV}^2}$ | $2.464^{+0.024}_{-0.048}$ | $-(2.464^{+0.024}_{-0.048})$ | $2.462^{+0.02}_{-0.04}$ | $-(2.462^{+0.003}_{-0.023})$ | | |
| $\sin^2 2\theta_{13}$ | $0.084^{+0.002}_{-0.002}$ | $0.084^{+0.003}_{-0.002}$ | $0.084^{+0.002}_{-0.003}$ | $0.084^{+0.002}_{-0.003}$ | | |
| $\sin^2 \theta_{23}$ | $0.55^{+0.03}_{-0.09}$ | $0.56^{+0.02}_{-0.03}$ | $0.44^{+0.02}_{-0.01} \oplus 0.58^{+0.02}_{-0.02}$ | $0.58^{+0.02}_{-0.02}$ | | |
| $\delta_{CP}/^\circ$ | $-(100^{+50}_{-60})$ | $-(90^{+30}_{-30})$ | $-(80.19^{+69.80}_{-36.21})$ | $-(86.50^{+38.62}_{-54.67})$ | | |
| $\frac{ a_{e\mu} }{10^{-23} \text{GeV}}$ | | | $1.86^{+2.57}_{-1.86}$ | 1.52 | < 4.80 | < 3.80 |
| $\frac{ a_{e\tau} }{10^{-23} \text{GeV}}$ | | | 0.57 | 4.16 | < 6.70 | < 9.50 |
| $\phi_{e\mu}/^\circ$ | | | -115.72 | 110.08 | | |
| $\phi_{e\tau}/^\circ$ | | | 84.36 | -89.27 | | |

TABLE IV: Parameter values at the best-fit points for the combined analysis of NO ν A and T2K. The 1σ error bars have been mentioned where possible. The 90% limits for 1 d.o.f have also been mentioned.

- [9] P. F. De Salas, S. Gariazzo, O. Mena, C. A. Ternes, and M. Tórtola, *Front. Astron. Space Sci.* **5**, 36 (2018), 1806.11051.
- [10] D. Ayres et al. (NO ν A) (2004), hep-ex/0503053.
- [11] Y. Itow et al. (T2K), pp. 239–248 (2001), hep-ex/0106019.
- [12] A. Himmel (2020), talk given at the Neutrino 2020 meeting on July, 2nd, 2020, <https://indico.fnal.gov/event/43209/contributions/187840/attachments/130740/159597/NOvA-Oscillations-NEUTRINO2020.pdf>.
- [13] P. Dunne (2020), talk given at the Neutrino 2020 meeting on July, 2nd, 2020, https://indico.fnal.gov/event/43209/contributions/187830/attachments/129636/159603/T2K_Neutrino2020.pdf.
- [14] K. J. Kelly, P. A. N. Machado, S. J. Parke, Y. F. Perez-Gonzalez, and R. Z. Funchal, *Phys. Rev. D* **103**, 013004 (2021), 2007.08526.
- [15] C. A. Argüelles et al., *Rept. Prog. Phys.* **83**, 124201 (2020), 1907.08311.
- [16] L. S. Miranda, P. Pasquini, U. Rahaman, and S. Razzaque (2019), 1911.09398.
- [17] S. S. Chatterjee and A. Palazzo, *Phys. Rev. Lett.* **126**, 051802 (2021), 2008.04161.
- [18] P. B. Denton, J. Gehrlein, and R. Pestes, *Phys. Rev. Lett.* **126**, 051801 (2021), 2008.01110.

- [19] V. A. Kostelecky and S. Samuel, Phys. Rev. D **39**, 683 (1989).
- [20] V. A. Kostelecky and S. Samuel, Phys. Rev. Lett. **63**, 224 (1989).
- [21] V. A. Kostelecky and R. Potting, Nucl. Phys. B **359**, 545 (1991).
- [22] V. A. Kostelecky and R. Potting, Phys. Rev. D **51**, 3923 (1995), hep-ph/9501341.
- [23] V. A. Kostelecky and R. Potting, Phys. Lett. B **381**, 89 (1996), hep-th/9605088.
- [24] M. Tanabashi et al. (Particle Data Group), Phys. Rev. D **98**, 030001 (2018).
- [25] T. Ohlsson and S. Zhou, Nucl. Phys. B **893**, 482 (2015), 1408.4722.
- [26] V. A. Kostelecky and M. Mewes, Phys. Rev. D **69**, 016005 (2004), hep-ph/0309025.
- [27] J. S. Diaz and A. Kostelecky, Phys. Rev. D **85**, 016013 (2012), 1108.1799.
- [28] V. A. Kostelecky and M. Mewes, Phys. Rev. D **70**, 076002 (2004), hep-ph/0406255.
- [29] T. Katori, V. A. Kostelecky, and R. Tayloe, Phys. Rev. D **74**, 105009 (2006), hep-ph/0606154.
- [30] A. Dighe and S. Ray, Phys. Rev. D **78**, 036002 (2008), 0802.0121.
- [31] G. Barenboim and J. D. Lykken, Phys. Rev. D **80**, 113008 (2009), 0908.2993.
- [32] B. Rebel and S. Mufson, Astropart. Phys. **48**, 78 (2013), 1301.4684.
- [33] A. de Gouvêa and K. J. Kelly, Phys. Rev. D **96**, 095018 (2017), 1709.06090.
- [34] G. Barenboim, C. A. Ternes, and M. Tórtola, Phys. Lett. B **780**, 631 (2018), 1712.01714.
- [35] G. Barenboim, M. Masud, C. A. Ternes, and M. Tórtola, Phys. Lett. B **788**, 308 (2019), 1805.11094.
- [36] R. Majhi, S. Chembra, and R. Mohanta, Eur. Phys. J. C **80**, 364 (2020), 1907.09145.
- [37] C. Giunti and M. Laveder, Phys. Rev. D **82**, 113009 (2010), 1008.4750.
- [38] A. Datta, R. Gandhi, P. Mehta, and S. U. Sankar, Phys. Lett. B **597**, 356 (2004), hep-ph/0312027.
- [39] A. Chatterjee, R. Gandhi, and J. Singh, JHEP **06**, 045 (2014), 1402.6265.
- [40] B. Singh Koranga and P. Khurana, Int. J. Theor. Phys. **53**, 3737 (2014).
- [41] J. S. Diaz and T. Schwetz, Phys. Rev. D **93**, 093004 (2016), 1603.04468.
- [42] D. Hooper, D. Morgan, and E. Winstanley, Phys. Rev. D **72**, 065009 (2005), hep-ph/0506091.
- [43] G. Tomar, S. Mohanty, and S. Pakvasa, JHEP **11**, 022 (2015), 1507.03193.
- [44] J. Liao and D. Marfatia, Phys. Rev. D **97**, 041302 (2018), 1711.09266.
- [45] S. Kumar Agarwalla and M. Masud, Eur. Phys. J. C **80**, 716 (2020), 1912.13306.
- [46] L. B. Auerbach et al. (LSND), Phys. Rev. D **72**, 076004 (2005), hep-ex/0506067.
- [47] P. Adamson et al. (MINOS), Phys. Rev. Lett. **101**, 151601 (2008), 0806.4945.

- [48] P. Adamson et al. (MINOS), *Phys. Rev. D* **85**, 031101 (2012), 1201.2631.
- [49] A. A. Aguilar-Arevalo et al. (MiniBooNE), *Phys. Rev. Lett.* **121**, 221801 (2018), 1805.12028.
- [50] Y. Abe et al. (Double Chooz), *Phys. Rev. D* **86**, 112009 (2012), 1209.5810.
- [51] K. Abe et al. (Super-Kamiokande), *Phys. Rev. D* **91**, 052003 (2015), 1410.4267.
- [52] M. G. Aartsen et al. (IceCube), *Nature Phys.* **14**, 961 (2018), 1709.03434.
- [53] K. Abe et al. (T2K), *Phys. Rev. D* **95**, 111101 (2017), 1703.01361.
- [54] V. A. Kostelecky and N. Russell (2008), 0801.0287.
- [55] A. Kostelecky and M. Mewes, *Phys. Rev. D* **85**, 096005 (2012), 1112.6395.
- [56] J. S. Diaz (2015), 1506.01936.
- [57] T. Kikuchi, H. Minakata, and S. Uchinami, *JHEP* **03**, 114 (2009), 0809.3312.
- [58] S. K. Agarwalla, S. S. Chatterjee, and A. Palazzo, *Phys. Lett. B* **762**, 64 (2016), 1607.01745.
- [59] M. Masud, S. Roy, and P. Mehta, *Phys. Rev. D* **99**, 115032 (2019), 1812.10290.
- [60] A. Cervera, A. Donini, M. B. Gavela, J. J. Gomez Cadenas, P. Hernandez, O. Mena, and S. Rigolin, *Nucl. Phys.* **B579**, 17 (2000), [Erratum: *Nucl. Phys.*B593,731(2001)], hep-ph/0002108.
- [61] L. Wolfenstein, *Phys. Rev.* **D17**, 2369 (1978).
- [62] P. Huber, M. Lindner, and W. Winter, *Comput.Phys.Commun.* **167**, 195 (2005), hep-ph/0407333.
- [63] P. Huber, J. Kopp, M. Lindner, M. Rolinec, and W. Winter, *Comput.Phys.Commun.* **177**, 432 (2007), hep-ph/0701187.
- [64] I. Esteban, M. C. Gonzalez-Garcia, A. Hernandez-Cabezudo, M. Maltoni, and T. Schwetz, *JHEP* **01**, 106 (2019), 1811.05487.
- [65] R. Nichol (MINOS) (2012), talk given at the Neutrino 2012 Conference, June 3-9, 2012, Kyoto, Japan, <http://neu2012.kek.jp/>.
- [66] H. Nunokawa, S. J. Parke, and R. Zukanovich Funchal, *Phys.Rev.* **D72**, 013009 (2005), hep-ph/0503283.